Proceedings of IMECE2007
2007 ASME International Mechanical Engineering Congress and Exposition
November 11-15, 2007, Seattle, Washington, USA

IMECE2007-41817

FUNCTIONAL ELECTRICAL STIMULATION OF A QUADRICEPS MUSCLE USING A NEURAL-NETWORK ADAPTIVE CONTROL APPROACH

Yan Tang
Department of Mechanical, Materials and Aerospace Engineering
University of Central Florida
Orlando, Florida 32816
tang36@gmail.com

Alexander Leonessa
Department of Mechanical, Materials and Aerospace Engineering
University of Central Florida
Orlando, Florida 32816
aleo@mail.ucf.edu

ABSTRACT

Functional electrical stimulation (FES) has been used to facilitate persons with paralysis in restoring their motor functions. In particular, FES-based devices apply electrical current pulses to stimulate the intact peripheral nerves to produce artificial contraction of paralyzed muscles. The aim of this work is to develop a model reference adaptive controller of the shank movement via FES. A mathematical model, which describes the relationship between the stimulation pulsewidth and the active joint torque produced by the stimulated muscles in non-isometric conditions, is adopted. The direct adaptive control strategy is used to address those nonlinearities which are linearly parameterized (LP). Since the torque due to the joint stiffness component is non-LP, a neural network (NN) is applied to approximate it. A backstepping approach is developed to guarantee the stability of the closed loop system. In order to address the saturation of the control input, a model reference adaptive control approach is used to provide good tracking performance without jeopardizing the closed-loop stability. Simulation results are provided to validate the proposed work.

1 Introduction

Functional electrical stimulation (FES) is a neuroprosthesis technique to restore motor function to individuals with spinal cord injuries (SCI) ([1]). For SCI patients, there are some muscles below the injury level which are still innervated, though not volitionally controllable. FES uses surface or implantable electrodes to generate current pulses in intact motor neurons to produce muscle contractions, generate joint torques and then the corresponding joint movements.

There are two kinds of FES control strategies: open-loop and closed-loop. Due to its simplicity, the open-loop FES has been used since 1960's ([1]). However, open-loop FES devices cannot adjust the output according to the actual effect and may require users' intensive support for balancing. By comparison, the closed-loop control has several advantages over the open-loop, such as better tracking performance and less sensitivity to modeling error and parameter variations ([2]). However, the classical feedback control has found very limited application in clinical use of FES since it cannot always guarantee the stability of the closed-loop system due to the challenges inherent in musculo-skeletal systems such as nonlinear characteristics, couplings, and time delay. Furthermore, muscles present highly nonlinear and time-varying characteristics when fatigue occurs and muscle model parameters are different for each individual ([3]). There is also a delay between stimulation and muscle contraction which adds to the processing and transmission delays in the electrical stimulation system ([4]).

To meet the requirement of advanced rehabilitation applica-

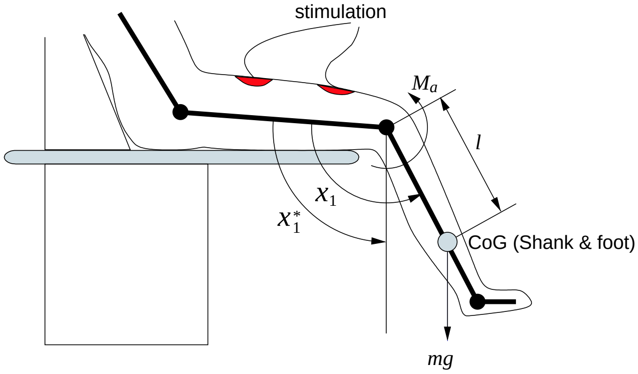

Figure 1. Knee-joint diagram ([13])

tions, a nonlinear closed-loop FES control system should be considered as it would allow to consider model uncertainties, as well as compensate for disturbances and unmodeled dynamics ([5]). Many closed-loop control strategies have been proposed in the literature including PID control ([6, 7]), artificial neural network control ([8, 9]), fuzzy controllers ([10]) and some nonlinear controllers ([11–13]). However, the existing control techniques cannot completely solve all the problems encountered in FES, such as lengthy tuning, time delays, inability to respond to changes due to muscle fatigue or external disturbance. Researchers are motivated to explore innovative methods to design more reliable and simpler FES equipment for possible clinical use.

In this paper, a neural network model reference adaptive controller (NN-MRAC) is applied on a physiological model developed in [14] in order to improve the tracking performance of the closed loop. The adoption of neural network avoids the need for information about the system nonlinear dynamics. The adaptive mechanism is based on Lyapunov stability theory which guarantees the tracking error is ultimately bounded. Numerical simulation results are presented to validate the controller.

2 Mathematical Model

The knee-joint tracking has been addressed numerous times in the literature (see for example [8, 12, 13, 15]) and this paper will consider the same benchmark problem. In this scenario, the thigh is stationary and only the shank-foot complex can move by stimulating the quadriceps muscle. In order to reduce the number of degrees of freedom, the ankle was fixed such that the ankle movement can be neglected. A nonlinear model developed in [14] of the electrically stimulated quadriceps muscle group has been adopted in this paper. In this model, the lower limb is modeled as an open kinematics chain composed of thigh and the shank-foot complex as shown in Figure 1. The input to this model is the pulsewidth of the current pulses, and the model output is the knee-joint kinematics.

The equation of the knee-joint motion under stimulation is described by ([14])

$$J\omega(t) = M_g(t) + M_e(t) + M_v(t) + M_a(t), \quad t \geqslant 0, \tag{1}$$

where J and $\omega(t)$ are the moment of inertia and the angular velocity of the shank-foot complex about the knee-joint, respectively. $M_g(t)$, $M_e(t)$ and $M_v(t)$ represent the gravitational moment, passive elastic moment and passive viscous moment, respectively, and are given by

$$M_g(t) = -mgl\sin\Big(x_1(t) - x_1^*\Big), \quad t \geqslant 0, \tag{2}$$

$$M_e(t) = -c_1\Big(x_1(t) - c_2\Big)e^{-c_3 x_1(t)}, \quad t \geqslant 0, \tag{3}$$

$$M_v(t) = -c_4 x_2(t), \qquad t \geqslant 0, \tag{4}$$

where m and l are the mass and the length of the shank-foot complex, $c_i, i = 1, \cdots, 4$ are unknown parameters, $x_1(t)$ and $x_2(t)$ represent the knee-joint angle and angular velocity, respectively. x_1^* is shown in Figure 1 and represents the angle between the thigh and the vertical direction in the sagittal plane. The relationship between pulsewidth and the active muscle torque $M_a(t)$ can be represented by a first order model whose transfer function is given by

$$H(s) = \frac{k^*}{1 + \tau^* s} \tag{5}$$

where τ^* is the time constant of this model and k^* is the static gain.

In this model, the parameters m, l and $c_i (i = 1, \cdots, 4)$ vary for different subjects and need to be identified. In order to design a direct adaptive controller, a state space model for the shank-quadriceps dynamics can be written as

$$\begin{aligned}
\dot{x}_1(t) &= x_2(t), \qquad\qquad x_1(0) = x_{10}, \quad t \geqslant 0,\\
\dot{x}_2(t) &= -\theta_1^* \sin(x_1(t) - x_1^*) + f(x_1(t))\\
&\quad -\theta_2^* x_2(t) + \theta_3^* x_3(t), \quad x_2(0) = x_{20}, \quad t \geqslant 0,\\
\dot{x}_3(t) &= -\theta_4^* x_3(t) + \theta_5^* u(t), \quad x_3(0) = x_{30}, \quad t \geqslant 0,
\end{aligned} \tag{6}$$

where $\theta_i^* \in \mathbb{R}$, $i = 1, \cdots, 5$ stand for real values of the unknown parameters of the model. Note that $\theta_i^* > 0$ because of their physical meanings.

3 Adaptive Controller Design

In this section, the neural network-model reference adaptive control law will be presented followed by the proof of stability.

Note that gravitational and viscous components are linearly parameterized (LP) while the elastic component is not LP, therefore, direct adaptive algorithm is developed to deal with the former while neural network is used to approximate the latter. A neural network with one 10-node hidden layer is adopted to approximate the elastic part in the knee kinematics as

$$M_{\mathrm{e}}(t) = W^{\mathrm{T}}(t)\sigma\Big(V^{\mathrm{T}}(t)x_1(t)\Big) + e_{\mathrm{NN}}(t), \tag{7}$$

where $W(t) \in \mathbb{R}^{10\times 1}$ and $V(t) \in \mathbb{R}^{1\times 10}$ are weight matrices, respectively, and their update laws are given as

$$\begin{aligned}\dot{W}(t) &= M\left[-e_2(t)\big(\sigma(V^{\mathrm{T}}(t)x_1(t)) - \sigma'(V^{\mathrm{T}}(t)x_1(t))V^{\mathrm{T}}(t)x_1(t)\big)\right. \\ &\quad \left. -k_{\mathrm{W}}e_2^2(t)W(t)\right], \quad W(0) = W_0, \quad t \geq 0, \qquad (8) \\ \dot{V}(t) &= N[-x_1(t)e_2(t)W^{\mathrm{T}}(t)\sigma'(V^{\mathrm{T}}(t)x_1(t)) - k_{\mathrm{V}}e_2^2(t)V(t)], \\ &\quad V(0) = V_0, \quad t \geq 0, \qquad (9)\end{aligned}$$

where $\sigma(\cdot)$ denotes the activation function and a sigmoid function is used in this paper. Furthermore, $M, N, k_{\mathrm{W}}, k_{\mathrm{V}} \in \mathbb{R}$, and $e_{\mathrm{NN}}(t)$ is the neural network approximation error.

3.1 Reference System

Note that there are thresholds and saturation phenomena in the motor recruitment ([16]). In other words, the stimulation pulsewidth has upper and lower bound limit. To ensure the stimulation stays in this range, a model reference system is developed such that the control system will track the reference trajectory rather than the desired trajectory. The reference system will provide a smooth convergence to the desired trajectory without control input (i.e. pulsewidth) beyond the controller saturation limit.

This reference system, composed of a combination of a second order oscillator and a filter, is given by

$$\begin{aligned}\dot{x}_{\mathrm{r}1}(t) &= x_{\mathrm{r}2}(t), \quad x_{\mathrm{r}1}(0) = x_{\mathrm{r}10}, \quad t \geqslant 0 \qquad (10) \\ \dot{x}_{\mathrm{r}2}(t) &= -\omega_0^2(x_{\mathrm{r}1}(t) - x_{\mathrm{r}1\mathrm{e}}) - 2\zeta\omega_0 x_{\mathrm{r}2}(t) \\ &\quad +\omega_0^2 x_{\mathrm{r}3}(t), \quad x_{\mathrm{r}2}(0) = x_{\mathrm{r}20}, \quad t \geqslant 0 \qquad (11) \\ \dot{x}_{\mathrm{r}3}(t) &= -\frac{1}{\tau}x_{\mathrm{r}3}(t) + \frac{k}{\tau}r(t), \quad x_{\mathrm{r}3}(0) = x_{\mathrm{r}30}, \quad t \geqslant 0 \qquad (12)\end{aligned}$$

where $x_{\mathrm{r}i}(t) \in \mathbb{R}$, $t \geq 0$, $i = 1,2,3$ are the states of the reference system and $[x_{\mathrm{r}1\mathrm{e}}, 0, 0]$ is the equilibrium of the reference system. The parameters ω_0 and ζ denote natural frequency and the damping coefficient of the oscillator, respectively. The construction of the reference system is motivated by the original system structure and the desired dynamics. The values for the parameters appearing in the reference system (ω_0, ζ, τ, k) are chosen as average values found in the literature. Next the reference system input $r(t)$ will be defined to guarantee the convergence of the reference system to the desired trajectory approximately.

Theorem 3.1. *Consider the reference system dynamics (10)-(12) and the tracking error $e(t)$ defined by*

$$e_{\mathrm{r}}(t) \triangleq \begin{bmatrix} e_{\mathrm{r}1}(t) \\ e_{\mathrm{r}2}(t) \\ e_{\mathrm{r}3}(t) \end{bmatrix} = \begin{bmatrix} x_{\mathrm{d}1}(t) - x_{\mathrm{r}1}(t) \\ x_{\mathrm{d}2}(t) - x_{\mathrm{r}2}(t) \\ x_{\mathrm{d}3}(t) - x_{\mathrm{r}3}(t) \end{bmatrix} \tag{13}$$

where $x_{\mathrm{d}1}(t) \triangleq x_{\mathrm{d}}(t)$, and $x_{\mathrm{d}2}(t)$, $x_{\mathrm{d}3}(t)$ are given by

$$\begin{aligned}x_{\mathrm{d}2}(t) &\triangleq \dot{x}_{\mathrm{d}}(t) + e_{\mathrm{r}1}(t), \qquad (14) \\ x_{\mathrm{d}3}(t) &\triangleq \frac{1}{\omega_0^2}\Big(\ddot{x}_{\mathrm{d}}(t) + \omega_0^2(x_{\mathrm{d}}(t) - x_{\mathrm{r}1\mathrm{e}}) + 2\zeta\omega_0\dot{x}_{\mathrm{d}}(t) \\ &\quad e_{\mathrm{r}1}(t) + \dot{e}_{\mathrm{r}1}(t)\Big), \qquad (15)\end{aligned}$$

along with the reference control input

$$r(t) = \frac{\tau}{k}\Big(\omega_0^2 e_{\mathrm{r}2}(t) + \dot{x}_{\mathrm{d}3}(t) + \frac{1}{\tau}x_{\mathrm{r}3}(t) + k_{\mathrm{r}}e_{\mathrm{r}1}(t)\Big). \tag{16}$$

The control command (16) guarantees asymptotical stability of the tracking error $e_{\mathrm{r}}(t)$.

Proof. Consider the Lyapunov function candidate

$$V_{\mathrm{r}}(e_{\mathrm{r}}) = \frac{1}{2}e_{\mathrm{r}1}^2 + \frac{1}{2}e_{\mathrm{r}2}^2 + \frac{1}{2}e_{\mathrm{r}3}^2. \tag{17}$$

Note that $V_{\mathrm{r}}(e_{\mathrm{r}})$ is $\mathcal{C}^1$ for all $e_{\mathrm{r}} \in \mathbb{R}^3$, $V_{\mathrm{r}}(e_{\mathrm{r}}) > 0$ for all $e_{\mathrm{r}} \in \mathbb{R}^3\backslash\{0\}$, and $V(0) = 0$.

Computing the time derivative of (17) and substituting (10)-(12) and (14)-(16), we obtain

$$\dot{V}_{\mathrm{r}}(t) = -e_{\mathrm{r}1}^2(t) - e_{\mathrm{r}2}^2(t) - e_{\mathrm{r}3}^2(t) \leq 0, \quad t \geq 0, \tag{18}$$

which is negative definite, proving the statement. □

Next, the controller that guarantees that the original system converges to the reference system will be developed.

3.2 Tracking Errors

The knee-joint is controlled to follow the desired knee-joint angle by stimulating the quadriceps using a PWM signal with suitable pulsewidth. Since this system has a strict feedback structure, a backstepping approach can be applied ([17]).

The position error is defined as

$$e_1(t) \triangleq x_{r1}(t) - x_1(t). \tag{19}$$

The following velocity error is generated by a backstepping procedure,

$$e_2(t) \triangleq x_{r2}(t) + k_1 e_1(t) - x_2(t), \tag{20}$$

where $k_1 > 0$.

Finally, the active torque tracking error is given by

$$e_3(t) = \chi_3(t) + \theta_7(t)\omega_0^2 x_{r3}(t) - x_3(t), \tag{21}$$

where $\theta_7(t)$ is the estimation of θ_3^* during the direct adaptive procedure, obtained from the update law

$$\dot{\theta}_7(t) = \Gamma_7\Big(e_2(t)\omega_0^2 x_{r3}(t) - k_{\theta_7} e_2^2(t)\theta_7(t)\Big), \quad \theta_7(0) = \theta_{70}, \quad t \geq 0, \tag{22}$$

with $\Gamma_7 > 0$, $k_{\theta_7} > 0$. The function $\chi_3(t)$ is obtained from the filter

$$T\dot{\chi}_3(t) + \chi_3(t) = \Theta_0^{\mathrm{T}}(t)\phi_0(t) - \theta_6(t)W^{\mathrm{T}}(t)\sigma(V^{\mathrm{T}}(t)x_1(t)) + k_{\alpha_3} e_2(t), \quad t \geqslant 0, \tag{23}$$

where $\Theta_0(t)$ is an estimate of $\Theta_0^* \triangleq \left[\, \frac{1}{\theta_3^*} \ \frac{\theta_1^*}{\theta_3^*} \ \frac{\theta_2^*}{\theta_3^*} \,\right]^{\mathrm{T}}$, and follows the update law

$$\dot{\Theta}_0(t) = \Gamma_0\Big(e_2(t)\phi_0(t) - k_{\theta_0} e_2^2(t)\Theta_0(t)\Big), \quad \Theta_0(0) = \Theta_{00}, \quad t \geq 0, \tag{24}$$

with $\Gamma_0 > 0$, $k_{\theta_0} > 0$. Furthermore,

$$\phi_0(t) = \begin{bmatrix} e_1(t) - \omega_0^2(x_{r1}(t) - x_{r1e}) - a_r x_{r2}(t) + k_1\dot{e}_1(t) + k_2 e_2(t) \\ -\sin(x_1(t) - x_1^*) \\ -x_2(t) \end{bmatrix}, \quad t \geq 0, \tag{25}$$

where $a_r \triangleq 2\zeta\omega_0$ and $k_2 > \frac{1}{2}$. $\theta_6(t)$ is also an estimation of θ_3^* and is obtained from the update law

$$\dot{\theta}_6(t) = \Gamma_6[-e_2(t)W^{\mathrm{T}}\sigma(V^{\mathrm{T}}(t)x_1(t)) - k_{\theta_6} e_2^2(t)\theta_6(t)], \quad \theta_6(0) = \theta_{60}, \quad t \geq 0, \tag{26}$$

where $\Gamma_6 > 0$, $k_{\theta_6} > 0$.

Remark. The filter (23) is used to solve the "explosion of terms" problem caused by the backstepping process. In order to simplify the controller, a technique derived from *Dynamic Surface Control* ([18]) is used.

During the directive adaptive control design procedure, there are two estimates to θ_3^*. Both estimates are independent and follow their respective update law.

3.3 Control Command

In this section, the control command $u(t) \in \mathbb{R}$ is defined to guarantee the tracking error is ultimately bounded, followed by the stability proof.

Theorem 3.2. *Consider the dynamical system (6) and the reference system dynamics (10)-(12), along with the tracking errors (19)-(21) and the control law*

$$u(t) \triangleq \Theta_1^{\mathrm{T}}(t)\phi_1(t), \quad t \geq 0 \tag{27}$$

where $\Theta_1(t) \in \mathbb{R}^{3\times 1}$ *is an estimate of* $\Theta_1^* \triangleq \left[\, \frac{1}{\theta_5^*} \ \frac{\theta_3^*}{\theta_5^*} \ \frac{\theta_4^*}{\theta_5^*} \,\right]^{\mathrm{T}}$, *and*

$$\phi_1(t) \triangleq \begin{bmatrix} \dot{\chi}_3(t) + \dot{\theta}_7(t)\omega_0^2 x_{r3}(t) + \theta_7(t)\omega_0^2\dot{x}_{r3}(t) + k_3 e_3(t) \\ e_2(t) \\ -x_3(t). \end{bmatrix} \tag{28}$$

Furthermore, the update law of $\Theta_1(t)$ *is given by*

$$\dot{\Theta}_1(t) = \Gamma_1\Big(e_3(t)\phi_1(t) - k_{\theta_1} e_3^2(t)\Theta_1(t)\Big), \quad \Theta_1(0) = \Theta_{10}, \quad t \geq 0, \tag{29}$$

where $\Gamma_1 > 0$, $k_{\theta_1} > 0$. *The control command (27) with update law (29) guarantees the convergence of* $(e, \tilde{\Theta}_f, \tilde{\Theta}, \tilde{\Theta}_1)$ *to the compact set*

$$\mathcal{M} \triangleq \Big\{(e, \tilde{\Theta}_f, \tilde{\Theta}, \tilde{\Theta}_1) : e^{\mathrm{T}}(t)Ke(t) \leq \frac{1}{2}\bar{\alpha}_{NN}^2 + \frac{1}{2}\bar{\alpha}_3^2 \\ \mathrm{tr}(\tilde{\Theta}_f^{\mathrm{T}}(t)\tilde{\Theta}_f(t)) \leq \mathrm{tr}(\tilde{\Theta}_f^{*\mathrm{T}}\tilde{\Theta}_f^*) \\ \mathrm{tr}(\tilde{\Theta}^{\mathrm{T}}(t)\tilde{\Theta}(t)) \leq \mathrm{tr}(\tilde{\Theta}^{*\mathrm{T}}\tilde{\Theta}^*) \\ \mathrm{tr}(\tilde{\Theta}_1^{\mathrm{T}}(t)\tilde{\Theta}_1(t)) \leq \mathrm{tr}(\tilde{\Theta}_1^{*\mathrm{T}}\tilde{\Theta}_1^*)\Big\}, \tag{30}$$

where $e(t) \triangleq \left[\, e_1(t) \ e_2(t) \ e_3(t) \,\right]^{\mathrm{T}}$, $K \triangleq \mathrm{diag}\left[\, k_1 \ k_2 - \frac{1}{2} \ k_3 \,\right]$, $\Theta(t) \triangleq \left[\, \Theta_0^{\mathrm{T}}(t) \ \theta_6(t) \ \theta_7(t) \,\right]^{\mathrm{T}}$, $\tilde{\Theta}_f(t) \triangleq \Theta_f(t) - \Theta_f^*$, $\tilde{\Theta}(t) \triangleq \Theta(t) - \Theta^*$, *and*

$$\Theta_f(t) \triangleq \begin{bmatrix} W(t) & 0_{10\times 10} \\ 0_{1\times 1} & V(t) \end{bmatrix}. \tag{31}$$

Furthermore, $\bar{\alpha}_3$ *is an upper bound to the filtering error* $\alpha_3(t)$ *given as*

$$\alpha_3(t) \triangleq \Theta_0^{\mathrm{T}}(t)\phi_0(t) - \theta_6(t)W^{\mathrm{T}}(t)\sigma(V^{\mathrm{T}}(t)x_1(t)) \\ -k_{\alpha 3}e_2(t) - \chi_3(t). \quad (32)$$

Proof. Consider the Lyapunov function candidate

$$V(e,\tilde{\Theta}_{\mathrm{f}},\tilde{\Theta},\tilde{\Theta}_1) \triangleq \frac{1}{2}e^{\mathrm{T}}e + \frac{1}{2}\mathrm{tr}(\tilde{\mathrm{W}}^{\mathrm{T}}\mathrm{M}^{-1}\tilde{\mathrm{W}}) + \frac{1}{2}\mathrm{tr}(\tilde{\mathrm{V}}^{\mathrm{T}}\mathrm{N}^{-1}\tilde{\mathrm{V}}) \\ + \frac{1}{2}\theta_3^* tr(\tilde{\Theta}^{\mathrm{T}}\Gamma^{-1}\tilde{\Theta}) + \frac{1}{2}\theta_5^* tr(\tilde{\Theta}_1^{\mathrm{T}}\Gamma_1^{-1}\tilde{\Theta}_1) \quad (33)$$

Note that $V(e,\tilde{\Theta}_{\mathrm{f}},\tilde{\Theta},\tilde{\Theta}_1)$ is $\mathcal{C}^1$ for all $e \in \mathbb{R}^3$, $\Theta_{\mathrm{f}} \in \mathbb{R}^{11\times 11}$, $\Theta \in \mathbb{R}^5$ and $\Theta_1 \in \mathbb{R}^3$, $V(e,\tilde{\Theta}_{\mathrm{f}},\tilde{\Theta},\tilde{\Theta}_1) > 0$ for all $(e,\tilde{\Theta}_{\mathrm{f}},\tilde{\Theta},\tilde{\Theta}_1) \in \mathbb{R}^3 \cup \mathbb{R}^{11\times 11} \cup \mathbb{R}^5 \cup \mathbb{R}^3 \backslash \{0\}$, and $V(0,0,0,0) = 0$.

When computing the derivative of (19) and substituting (20), we obtain

$$\dot{e}_1(t) = -k_1 e_1(t) + e_2(t), \quad t \geq 0. \quad (34)$$

Similarly, the derivative of (20) can be obtained as

$$\dot{e}_2(t) = \dot{x}_{\mathrm{r}2}(t) + k_1\dot{e}_1(t) - \dot{x}_2(t), \quad t \geq 0. \quad (35)$$

The time derivative of the Lyapunov function can be obtained using the update laws (8), (9), (22), (24), (26) and (29) as

$$\dot{V}(t) = -e^{\mathrm{T}}Ke(t) - k_{\mathrm{W}}e_2^2(t)\mathrm{tr}(\tilde{W}^{\mathrm{T}}(t)W(t)) \\ -k_{\mathrm{V}}e_2^2(t)\mathrm{tr}(\tilde{V}^{\mathrm{T}}(t)V(t)) + e_2(t)e_{\mathrm{NN}}(t) \\ -k_{\Theta_1}e_3^2(t)\theta_5^*\tilde{\Theta}_1^{*\mathrm{T}}\tilde{\Theta}_1^* - \theta_3^* k_{\alpha_3}e_2^2(t), \\ V(0) = V_0, \quad t \geq 0. \quad (36)$$

By completion of the square, (36) can be written as

$$\dot{V}(t) = -e^{\mathrm{T}}(t)Ke(t) - k_{\mathrm{W}}e_2^2(t)\mathrm{tr}(\tilde{\mathrm{W}}^{\mathrm{T}}(\mathrm{t})\mathrm{W}(\mathrm{t})) \\ -k_{\mathrm{V}}e_2^2(t)\mathrm{tr}(\tilde{\mathrm{V}}^{\mathrm{T}}(\mathrm{t})\mathrm{V}(\mathrm{t})) - \frac{1}{2}\left(\mathrm{e}_2(\mathrm{t}) - \mathrm{e}_{\mathrm{NN}}(\mathrm{t})\right)^2 \\ +\frac{1}{2}e_2^2(t) + \frac{1}{2}e_{\mathrm{NN}}^2(t) - k_{\Theta}e_2^2(t)\theta_3^* \\ -\frac{1}{2}\left(\theta_3^* e_2(t) - \alpha_3(t)\right)^2 + \frac{1}{2}\theta_3^{*2}e_2^2(t) \\ +\frac{1}{2}\alpha_3^2(t) - k_{\Theta_1}e_3^2(t)\theta_5^*\tilde{\Theta}_1^{*\mathrm{T}}\tilde{\Theta}_1^* - \theta_3^* k_{\alpha_3}e_2^2(t), \\ V(0) = V_0, \quad t \geq 0. \quad (37)$$

Since $\|\alpha_3(t)\| < \bar{\alpha}$, $\|e_{\mathrm{NN}}(t)\| < \bar{e}_{\mathrm{NN}}$, $t \geq 0$, choose $k_{\alpha_3} > \frac{1}{2}\theta_3^*$ and there exits the upper bound on $\dot{V}$,

$$\dot{V}(t) \leq -e^{\mathrm{T}}(t)Ke(t) + \frac{1}{2}\bar{e}_{\mathrm{NN}}^2 + \frac{1}{2}\bar{\alpha}_3^2 \\ +\frac{k_{\mathrm{W}}e_2^2(t)}{2}(W^{*\mathrm{T}}W^* - \tilde{W}^{\mathrm{T}}(t)\tilde{W}(t)) \\ +\frac{k_{\mathrm{V}}e_2^2(t)}{2}\mathrm{tr}(V^{*\mathrm{T}}V^* - \tilde{V}^{\mathrm{T}}(t)\tilde{V}(t)) \\ +\frac{k_{\Theta}e_2^2(t)\theta_3^*}{2}\mathrm{tr}(\Theta^{*\mathrm{T}}\Theta^* - \tilde{\Theta}^{\mathrm{T}}(t)\tilde{\Theta}(t)), \quad (38)$$

which guarantees the convergence of $(e,\tilde{\Theta}_{\mathrm{f}},\tilde{\Theta},\tilde{\Theta}_1)$ to the compact set (30). □

3.4 Adaptive Control with Actuator Amplitude Saturation Constraint

In this section, the adaptive control design will be extended to account for the actuator amplitude saturation. According to the muscles activation dynamics, the stimulation pulsewidth should be limited between $\mathrm{pw}_{\mathrm{thr}}$ and $\mathrm{pw}_{\mathrm{sat}}$, where $\mathrm{pw}_{\mathrm{thr}}$ represents the pulsewidth for which the first motor units are recruited and $\mathrm{pw}_{\mathrm{sat}}$ is the maximum pulsewidth to recruit all the muscle motor units ([16]). According to Theorem 3.2, the control law (27) guarantees an ultimately bounded tracking error. Note that the control input $u(t)$, $t \geq 0$, depends on the reference system input $r(t)$, $t \geq 0$, through $\dot{x}_{\mathrm{r}3}(t)$, $t \geq 0$, which means that the amplitude of $u(t)$, $t \geq 0$, can be adjusted using the reference input $r(t)$ which will also affect the reference system. The reference system state $x_{\mathrm{r}}(t) \in \mathbb{R}^{3\times 1}$ is uniquely determined by $r(t)$, $t \geq 0$, for any given initial condition. Next, we will show how the reference system input $r(t)$, $t \geq 0$, can be used to guarantee an ultimately bounded tracking error in the face of actuator amplitude saturation.

The control law (27) can be rewritten as

$$u(t) = \Theta_1^{\mathrm{T}}(t)\bar{\phi}_1(t) + \Theta_{11}(t)\theta_7(t)\omega_0^2\dot{x}_{\mathrm{r}3}(t), \quad t \geq 0, \quad (39)$$

where $\Theta_{11}(t)$ is the first component of $\Theta_1(t)$ and

$$\bar{\phi}_1(t) = \begin{bmatrix} \dot{\chi}_3(t) + \dot{\theta}_7(t)\omega_0^2 x_{\mathrm{r}3}(t) + k_3 e_3(t) \\ e_2(t) \\ -x_3(t). \end{bmatrix}. \quad (40)$$

In order to satisfy $pw_{\mathrm{thr}} \leq u(t) \leq pw_{\mathrm{sat}}$, $\dot{x}_{\mathrm{r}3}(t)$ must be limited such that $\dot{x}_{\mathrm{r}3_{\mathrm{thr}}} \leq \dot{x}_{\mathrm{r}3} \leq \dot{x}_{\mathrm{r}3_{\mathrm{sat}}}$, where

$$\dot{x}_{\mathrm{r}3_{\mathrm{thr}}} = \frac{u_{\mathrm{thr}} - \Theta_1^{\mathrm{T}}\bar{\phi}_1(t)}{\Theta_1(t)(1)\theta_7(t)\omega_0^2}, \quad t \geq 0, \quad (41)$$

$$\dot{x}_{\mathrm{r}3_{\mathrm{sat}}} = \frac{u_{\mathrm{sat}} - \Theta_1^{\mathrm{T}}\bar{\phi}_1(t)}{\Theta_1(t)(1)\theta_7(t)\omega_0^2}, \quad t \geq 0, \quad (42)$$

are obtained from (39) and (40). Since the reference system is a known system and its dynamics can be changed as needed, we can use (16) together with (41) and (42) to obtain the reference input $r(t)$ which guarantees that the input pulsewidth (27) does not exceed the saturation limit.

4 Simulation Results

The simulations were performed using Runge-Kutta solver and integration time-step of 10 ms. The shank movement is controlled to follow a sinusoidal reference signal $x_{\mathrm{d}}(t)$ varying between 125 and 135 degree with a frequency of 0.5 Hz. The parameters used in the simulation are given in Table 1. The gains are arbitrarily chosen to be $k_1 = k_2 = k_3 = k_{\mathrm{r}} = 10$, and $\Gamma_i = 0.1, i = 0, 1, 6, 7$.

The initial conditions for the simulation are given as $\begin{bmatrix} x_{10} \; x_{20} \; x_{30} \end{bmatrix} = \begin{bmatrix} x_{\mathrm{r}10} \; x_{\mathrm{r}20} \; x_{\mathrm{r}30} \end{bmatrix} = \begin{bmatrix} 2.26 \; 0.27 \; 0 \end{bmatrix}$, $W_0 = 0_{10\times1}$, $V_0 = 0_{1\times10}$.

Table 1: Parameters used in the simulation

m(kg)	l(m)	J(kgm^2)	$c_1(\frac{\mathrm{Nms}}{\mathrm{rad}})$	c_2(rad)
4.37	0.238	0.362	41.208	2.918
$c_3(\frac{1}{\mathrm{rad}})$	$c_4(\frac{\mathrm{Nm}}{\mathrm{rad}})$	τ(s)	$G(\frac{\mathrm{Nm}}{\mathrm{s}})$	r_{r1e}(rad)
5.591	0.27	0.951	0.014	1.8
$\omega_0(\frac{1}{\mathrm{s}})$	ζ	x_1^*(rad)		
38.67	0.01	1.66		

The simulation results of the control input without considering input saturation are shown in Figure 2. Since the saturation has not been taken into account, the control algorithm does not generate meaningful pulsewidth. As shown in Figure 2, the pulsewidth assumes negative values, which is not physically possible. When we include the saturation algorithm, we obtain the results shown in Figure 3. In this case the system converges smoothly to the desired trajectory, without exceeding the pulsewidth saturation limits.

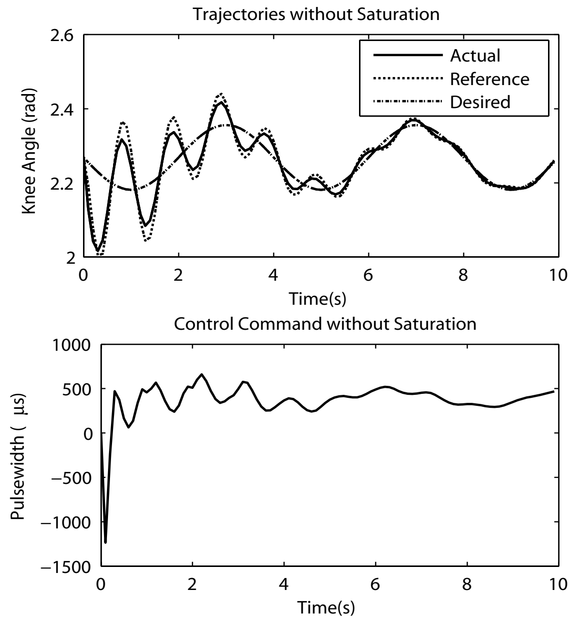

Figure 2. **Tracking control without Saturation.**

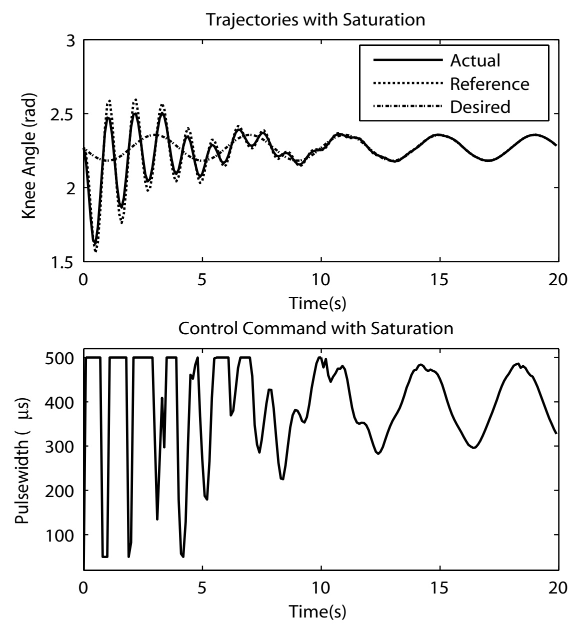

Figure 3. **Tracking control using NN-MRAC.**

5 Conclusions

A neural network-model reference adaptive controller was investigated for the shank-foot complex movement using FES. Lyapunov stability analysis was provided to guarantee an ultimately bounded tracking error. The introduction of a reference system also ensures that the stimulation pulsewidth satisfies the muscle recruitment limit. Simulation results are presented to validate the controller design.

REFERENCES

[1] A. Kralj and T. Bajd, *Functional Electrical Stimulation: Standard and Walking after Spinal Cord Injury*. CRC Press, 1989.

[2] P. E. Crago, J. T. Mortimer, and P. Peckham, “Closed-loop

control of force during electrical stimulation of muscle," *IEEE Transactions on Biomedical Engineering*, pp. 306–312, 1988.

[3] H. B. K. Boom, A. J. Mulder, and P. H. Veltink, "Fatigue during functional neuromuscular stimulation," *Progress in Brain Research*, pp. 409–418, 1993.

[4] C. Lynch and M. Popovic, "Closed-loop control for FES: Past work and future directions," in *Annual Conference of International FES Society*, 2005.

[5] H. J. Chizeck, "Adaptive and nonlinear control methods for neural prosthesis," in *Neural prostheses - replacing motor function after disease or disability* (R. Stein, H. Peckham, and D. Popovic, eds.), New York: Oxford University Press, 1992.

[6] H. J. Chizeck, N. Lan, L. S. Palmieri, and P. E. Crago, "Feedback control of electrically stimulated muscle using simultaneous pulse width and stimulus period modulation," *Biomedical Engineering, IEEE Transactions on*, pp. 1224–1234, 1991.

[7] T. Watanabe, T. Matsudaira, K. Kurosawa, T. Fujii, R. Futami, N. Hoshimiya, and M. Ichie, "Wrist joint control by multichannel closed-loop FES system: System improvement and first clinical test," in *Annual Conference of the International Functional Electrical Stimulation Society*, 2002.

[8] C. Gwo-Ching, L. Jer-Junn, L. Gon-Der, L. Jin-Shin, C. Cheng-Kung, K. Bor-Lin, and K. Te-Son, "A neurocontrol system for the knee joint position control with quadriceps stimulation," *IEEE Transactions on Rehabilitation Engineering*, pp. 2–11, 1997.

[9] M. M. Adamczyk and P. E. Crago, "Simulated feedforward neural network coordination of hand grasp and wrist angle in a neuroprosthesis," *Rehabilitation Engineering, IEEE Transactions on [see also IEEE Trans. on Neural Systems and Rehabilitation]*, pp. 297–304, 2000.

[10] J. J. Chen, Y. Nan-Ying, H. Ding-Gau, A. Bao-Ting, and C. Gwo-Ching, "Applying fuzzy logic to control cycling movement induced by functional electrical stimulation," *IEEE Transactions on Rehabilitation Engineering*, pp. 158–169, 1997.

[11] F. Previdi and E. Carpanzano, "Design of a gain scheduling controller for knee-joint angle control by using functional electrical stimulation," *IEEE Transactions on Control Systems Technology*, pp. 310–324, 2003.

[12] S. Jezernik, R. G. V. Wassink, and T. Keller, "Sliding mode closed-loop control of FES controlling the shank movement," *Biomedical Engineering, IEEE Transactions on*, pp. 263–272, 2004.

[13] T. Schauer, N. O. Negard, F. Previdi, K. J. Hunt, M. H. Fraser, E. Ferchland, and J. Raisch, "Online identification and nonlinear control of the electrically stimulated quadriceps muscle," *Control Engineering Practice*, pp. 1207–1219, 2005.

[14] M. Ferrarin and A. Pedotti, "The relationship between electrical stimulus and joint torque: a dynamic model," *Rehabilitation Engineering, IEEE Transactions on [see also IEEE Trans. on Neural Systems and Rehabilitation]*, vol. 8, no. 3, pp. 342–352, 2000.

[15] M. S. Hatwell, B. J. Oderkerk, C. A. Sacher, and G. F. Inbar, "The development of a model reference adaptive controller to control the knee joint of paraplegics," *Automatic Control, IEEE Transactions on*, pp. 683–691, 1991.

[16] R. Riener and T. Fuhr, "Patient-driven control of FES-supported standing up: a simulation study," *IEEE Transactions on Rehabilitation Engineering*, vol. 6, no. 2, pp. 113–124, 1998.

[17] H. K. Khalil, *Nonlinear Systems*. Prentice-Hall, Upper Saddle River, NJ, 1996.

[18] D. Swaroop, J.-K. Hedrick, P.-P. Yip, and J.-C. Gerdes, "Dynamic surface control for a class of nonlinear systems," *IEEE Trans. Autom. Contr.*, vol. 45, pp. 1893–1899, 2000.